

# OPTIMIZATION OF A FLAT DIE GEOMETRY

Y. Sun and M. Gupta

Mechanical Engineering-Engineering Mechanics Department  
Michigan Technological University  
Houghton, MI 49931

## Abstract

Geometry of a flat die for polymer sheet extrusion is optimized to obtain a uniform velocity distribution across the exit of the die. While optimizing the exit velocity distribution, the constraint optimization algorithm used in this work enforced a limit on the maximum allowable pressure drop in the die. Effect of the shear as well as elongational viscosity of the polymer on the flow in the flat die is taken into account.

## Introduction

Flat die (Fig. 1) is commonly used to extrude thin sheet of plastics [1, 2]. The flow channel cross-section at the entrance of a flat die is typically a circle or a rectangle with a small aspect ratio. In a flat die, this initial cross-section is gradually transformed to a large aspect ratio rectangle required for sheet extrusion. However, if the channel geometry in a flat die is not designed properly the velocity at the exit of the flat die may not be uniform. A non-uniform velocity distribution at the die exit may lead to a variation in the sheet thickness across the width of the die. Since a tight control on thickness is required for a high quality plastic sheet, the main goal in design of a flat die is to optimize the die channel geometry such that a uniform velocity distribution is obtained at the die exit [3 – 9]. The flow obstruction provided by the thin and long land near the exit of a flat die increases the uniformity of the velocity distribution at the exit. In general, uniformity of the exit velocity can be improved by increasing the length of the die land. However, an increase in land length rapidly increases the pressure drop across the die if the same flow rate is maintained or rapidly decreases the flow rate for a fixed pressure drop across the die. Therefore, channel geometry of a flat die should be optimized such that a uniform velocity distribution at the die exit is obtained without excessively increasing the pressure drop across the die. The complexity of the polymer rheology further increases the difficulty of the die optimization problem. If the rheology of a polymer is not accounted accurately while optimizing the die, the predicted velocity, pressure and temperature fields are expected to have large errors, which may result in a suboptimal die design. The diversity in the rheology of different polymers also necessitates individual optimization of the die for each polymer. A suboptimal combination of polymer and die channel

geometry often requires supplementary equipment such as chocker bar [1, 2] to obtain a uniform velocity at the die exit. Such a trial and error approach is not only expensive, but also increases the pressure drop across the die.

In the present work, a software for optimization of the geometry of flat dies has been developed. This software uses the PELDOM software [10] for a three dimensional simulation of the flow in extrusion dies. To simulate a non-isothermal polymeric flow, the flow simulation software accounts for the strain-rate- and temperature-dependence of the shear as well as the elongational viscosity of the polymer [11 – 15]. The viscosity models and the values of the various parameters in these models for the polymer used in the present work are summarized in the next section.

## Material Properties of the Polymer

In the present work, geometry of a flat die was optimized for a low-density polyethylene (Dow 132i). To capture the strain-rate dependence of the shear ( $\eta_s$ ) and elongational ( $\eta_e$ ) viscosities of the polymer, the Carreau model (Eqn. 1) [16] and the Sarkar-Gupta model (Eqn. 2) [13], respectively, were used in this work:

$$\eta_s = \eta_0 (1 + (\lambda e_{II})^2)^{\frac{n-1}{2}} \quad (1)$$

$$\eta_e = \eta_0 \left[ T_r + \delta \left\{ 1 - \frac{1}{\sqrt{1 + (\lambda_1 e_{II})^2}} \right\} \right] (1 + (\lambda_2 e_{II})^2)^{\frac{m-1}{2}} \quad (2)$$

where,  $e_{II} = \sqrt{2(\tilde{\epsilon} : \tilde{\epsilon})}$  is the second invariant of the strain-rate tensor  $\tilde{\epsilon} = (\nabla \hat{v} + \nabla \hat{v}^T)/2$ , with  $\hat{v}$  being the velocity,  $T_r$ , the Trouton ratio at low strain rates, is 3 for an axisymmetric flow and 4 for a planar flow, and  $\eta_0, \delta, \lambda, \lambda_1, \lambda_2, n$  and  $m$  are material parameters.

The Arrhenius model [16] was used for temperature dependence of the zero-shear viscosity:

$$\eta_0 = A \exp(T_a / T) \quad (3)$$

where,  $T$  is the temperature of the polymer, and  $A$  and  $T_a$  are material parameters. The temperature dependence of  $\lambda, \lambda_1$  and  $\lambda_2$  were obtained by using the time-temperature superposition principle along with the Arrhenius model

(Eqn. 3). Values of various shear and elongational viscosity parameters were given in references [15, 17].

The thermal conductivity ( $K$ ), density ( $\rho$ ) and heat capacity ( $C_p$ ) of the polymer were assumed to be constant for the range of temperature in the flat dies. Since the actual values of  $K$ ,  $\rho$  and  $C_p$  for Dow 132i were not known, typical values of these parameters for a low-density polyethylene ( $K = 0.25$  W/m K,  $\rho = 740$  kg/m<sup>3</sup>,  $C_p = 2300$  J/kg K), were used for the flow simulation.

### Optimization of the Channel Geometry of a Flat Die: Problem Formulation

It was mentioned earlier that the goal in design of a flat die is to minimize the velocity variation across the die exit without excessively increasing the pressure drop in the die. This can be formulated as a constrained optimization problem as follows.

$$\text{Minimize } V(x) = \sqrt{\frac{1}{N} \cdot \sum_{i=1}^N \|v_i - \bar{v}\|^2} \quad (4)$$

$$\text{such that } P(x) \leq P_0 \quad (5)$$

where  $i$  denotes a node at the die exit,  $N$  is the total number of nodes at the die exit,  $v_i$  is the velocity at an exit node,  $\bar{v}$  is the average exit velocity,  $P$  is the pressure drop across the die,  $P_0$  is the specified limit for the pressure drop across the die, and  $x$  is a set of the die geometry parameters, which are to be optimized.

As discussed before, in general a more uniform velocity distribution can be obtained at the die exit if the limit for the pressure drop across the die is increased. Accordingly, for the optimum die geometry the pressure drop across the die is expected to be the specified pressure limit  $P_0$ . Since an equality constraint is easier to implement than an inequality constraint in an optimization problem, in the present work, the inequality in Eqn. (5) was implemented as an equality constraint:  $P(x) = P_0$ . To enforce this pressure constraint, the quadratic penalty method was used in this work [18]. The modified objective function thus obtained is

$$f(x) = V(x) + \frac{1}{\mu} G(x) \quad (6)$$

where

$$G(x) = (P(x) - P_0)^2 \quad (7)$$

and  $\mu$  is the penalty parameter. Typically, in the quadratic penalty method, to closely satisfy the constraint, the value of  $\mu$  is reduced in each optimization iteration. However, the optimization problem gets ill conditioned as  $\mu \rightarrow 0$ , resulting in severe numerical difficulties as  $\mu$  becomes

small. Furthermore, the goal in the present work is not to satisfy the pressure constraint exactly, but to make sure that the pressure drop across the die does not increase excessively beyond the specified limit. Therefore, instead of decreasing the penalty parameter in each iteration, a constant value, given below, was used.

$$\frac{1}{\mu} = 100 \cdot \frac{V(x^{(0)})}{P_0^2} \quad (8)$$

where  $V(x^{(0)})$  is the value of  $V(x)$  for the initial die design. With this value of the penalty parameter, the value the pressure penalty term in Eqn. (6) is equal to that of the velocity variation term when  $|P(x) - P_0|/P_0 = 0.1$ . It was found that the value of penalty parameter in Eqn. (8), enforces the pressure constraint with a reasonable accuracy and also avoids the ill-conditioning of the quadratic penalty method.

In the present work, the geometry of a flat die was defined by nineteen geometric parameters. For the die shown in Fig. 1, the values of these parameters, which were taken from reference [5], are given in table 1. Out of these nineteen parameters, some of the parameters (die width, manifold center depth, inlet length, inlet width, and land gap in center) are fixed and are given as design specifications. Some of the remaining parameters (preland side length, manifold backwall angel, manifold angle, and secondary manifold angle) were found to have only a minimal effect on the exit velocity distribution and on the pressure drop in the die. Therefore, to improve the efficiency of the optimization algorithm, the values of these parameters in the initial design were left unaltered during the design space exploration in the optimization problem. To further reduce the number of design variables, the secondary manifold center length was set to the same value as that of the secondary manifold side length. Therefore, only the values of nine geometric parameters are optimized in this work to minimize the velocity variation at the die exit. The BFGS optimization algorithm [18], which is a quasi-Newtonian optimization method, was used in this work.

### Optimization of the Channel Geometry of a Flat Die: Results and Discussion

The optimization scheme described in the last two sections along with the material properties given in reference [15] were used to optimize a flat die for Dow132i. The design of the flat die based upon the values of the various geometric parameters given in table 1, which are taken from reference [5], was employed as the initial design for the optimization scheme.

A flow rate of  $2.56 \times 10^{-4}$  m<sup>3</sup>/s was specified at the entrance, and the temperatures at the die wall and at the die entrance were 473 and 503 K. Effect of the high elongational viscosity of polymer on the flow in this initial die design has already been analyzed in our earlier

publication [15]. By comparing the flow simulation including the effect of elongational viscosity with the simulation using a generalized Newtonian formulation, we found that the elongational viscosity has large effect on the pressure and temperature distributions in this die. In particular, when the effect of elongational viscosity was included in the simulation, the predicted pressure drop in the die increased by 17%, whereas the temperature at the die exit increased by about 8 °C.

For the initial die design, the velocity, pressure and temperature distributions at the mid-plane of the die are shown in Fig. 3 (a), 4 (a) and 5 (a). Figs. 3 – 5 also show the velocity, pressure and temperature distributions for two other flat die designs obtained during the iterative optimization process. Figs. 3 (b), 4 (b) and 5 (b) show the velocity, pressure and temperature distributions for a design obtained at an intermediate optimization iteration, whereas the distribution in Fig. 3 (c), 4 (c) and 5 (c) are for the final optimized design. The velocity, pressure and temperature distributions in Fig. 3 – 5 were obtained by including the effect of elongational viscosity of Dow 132i. The values of the nine geometric variables for the intermediate and optimized die are given in Table 1.

Qualitatively, the velocity distributions at the exit of the intermediate and optimized dies in Fig. 3 (b) and (c) are more uniform than the exit velocity in the initial die design in Fig. 3 (a). For a quantitative comparison, Fig. 6 shows the mid-plane velocity across the exit of the die. It is evident from Fig. 6 that in the initial die design, the exit velocity in the middle one-third of the die is significantly higher than the velocity in the two one-third portions of the die near the two ends. In Fig. 6, the exit velocity distributions for the intermediate and optimized die designs are much more uniform across the complete width of the die. Only in the small regions near the two ends of these two dies, the exit velocity reduces to zero to satisfy the no-slip condition at the walls.

The pressure drop in the initial die design was specified as the pressure drop limit,  $P_0$ , in the optimization algorithm. That is, the goal was to improve the uniformity of exit velocity without increasing the pressure drop in the die. It should be noted that even though the values of various geometric parameters in Table 1 are significantly different for the three dies, the pressure drops across the three dies in Fig. 4 are almost the same. To improve the uniformity of die exit velocity, the length of the land near the exit is typically increased. Against this general practice in flat die design, the optimization program in fact reduced the land length. Since the total pressure drop in the die was enforced to remain unchanged by the pressure constraint, the reduction in pressure drop in the land for a smaller land length, allowed the change in the various geometric parameters for the manifold, preland and secondary manifold without increasing the total pressure drop in the die. To obtain a uniform velocity distribution at the exit, the dimensions of the preland and secondary manifold in

the thickness direction were reduced, whereas, the axial dimension of the manifold as well as that of the preland was decreased. In particular, secondary manifold depth was reduced by almost 50%, preland gap was reduced by 7%, whereas, preland center length and manifold center flat length were increased by 45% and 10%, respectively. The changes in these four dimensions increased the pressure drop in the manifold, preland and secondary manifold, but this increase in pressure drop was compensated by the reduction in pressure due to a smaller land length. Other dimensions, which are changed significantly by the optimization algorithm, are manifold side depth and manifold end sweep length. The increase in the manifold side depth and manifold end sweep length, probably does not affect the pressure drop significantly, but helps in distributing the polymer across the die width as it comes out of the inlet channel.

Instead of having a uniform exit temperature distribution, all three temperature distributions in Fig. 5 have bands of high and low temperatures. Such temperature bands are often observed in sheet extrusion. However, it is noted that since more polymer is flowing towards the two ends of the intermediate and optimized dies (see Fig. 6), in comparison to the shear heating in the initial die (Fig. 5 (a)), the shear heating, and hence, the temperature in the intermediate and optimized dies (Fig. 5(b) and (c)) is lower near the middle of the die and higher near the ends.

## Conclusions

A software for optimizing the geometry of a flat die for polymer sheet extrusion has been developed. The optimization software used the PELDOM software to simulate the polymeric flow in the flat die. The software developed in this work successfully optimized the geometry of a flat die such that a uniform velocity distribution was obtained at the die exit, without increasing the pressure drop in the die.

## Acknowledgement

This work was supported by the National Science Foundation Grant DMI-0200091.

## References

1. P. N. Richardson, *Introduction to Extrusion*, Society of Plastics Engineers, Brookfield, CT (1974).
2. W. Michaelli, *Extrusion Dies for Plastics and Rubber*, Hanser Publishers, New York (1992).
3. W. A. Gifford, *SPE ANTEC Tech. Papers*, **44**, 290 (1998).
4. J. M. Nobrega, O. S. Carneiro, F. T. Pinho, and P. J. Oliveira, *SPE ANTEC Tech. Papers*, **47**, 59 (2001).

5. W. A. Gifford, *Poly. Eng. Sci.*, **41**, 1886 (2001).  
6. J. M. Nobrega, O. S. Carneiro, F. T. Pinho, P. J. and Oliveira, *SPE ANTEC Tech. Papers*, **48**, 122 (2002).  
7. S. Kaul, and W. Michali, *SPE ANTEC Tech. Papers*, **48**, 131 (2002).  
8. W. A. Gifford, *SPE ANTEC Tech. Papers*, **48**, 147 (2002).  
9. L. G. Reifschneider, *SPE ANTEC Tech. Papers*, **48**, 151 (2002).  
10. PELDOM software, Plastic Flow, LLC, 1206 Birch Street, Houghton, MI 49931.  
11. M. Gupta, *Poly. Eng. Sci.*, **40**, 23 (2000).  
12. M. Gupta, *J. Reinf. Plast. Comp.*, **20**, 341 (2001).  
13. D. Sarkar and M. Gupta, *J. Reinf. Plast. Comp.*, **20**, 1473 (2001).  
14. M. Gupta, *J. Reinf. Plast. Comp.*, **20**, 1464 (2001).  
15. Y. Sun and M. Gupta, *SPE ANTEC Tech. Papers*, **49**, 290 (2003).  
16. R. B. Bird, R. C. Armstrong and O. Hassager, *Dynamics of Polymeric Liquids*, Vol. 1 and 2, Wiley, New York (1987).  
17. P. Beaupre and M. Gupta, *Int. Polym. Proc. Journal*, **17**, 370 (2002).  
18. J. Nocedal, and S. J. Wright, *Numerical Optimization*, Springer-Verlag, New York (1999).

Key Words: Extrusion, Die design, Optimization, Elongational viscosity, LDPE.

Table 1 Geometric parameters for the three different flat die geometries.

Lengths	Initial (cm)	Intermediate (cm)	Optimized (cm)
Preland gap	0.61	0.50	0.57
Preland center length	5.08	6.34	7.39
Secondary manifold center length	5.08	5.15	5.09
Secondary manifold side length	5.08	5.15	5.09
Secondary manifold depth	0.635	0.51	0.32
Land length	2.54	2.47	2.20
Manifold side depth	1.02	1.18	1.34
Manifold center flat length (including radius)	1.52	1.64	1.68
Manifold side flat length (including radius)	1.02	1.02	1.02
Manifold end sweep length	10.16	12.38	12.48
Values of parameters which remained unchanged during the optimization			
Lengths	cm	Angles	degrees
Die width	101.6	Manifold backwall angle	85
Die length (including channel)	33.0	Manifold angle	20
Inlet width	10.16	Secondary manifold angle	20
Manifold center depth	3.81		
Preland side length	0.00254		
Land gap in center	0.102		

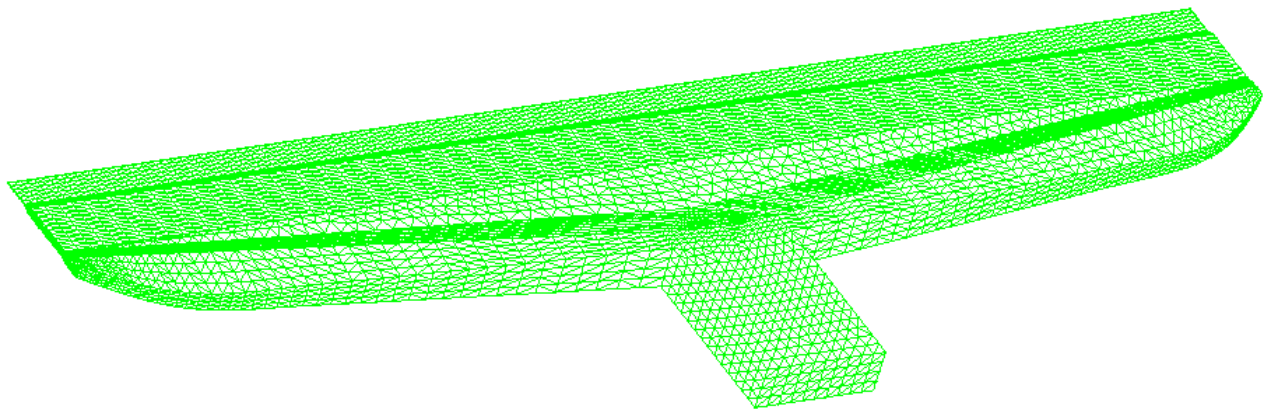


Fig. 1 Finite element mesh in the initial flat die design.

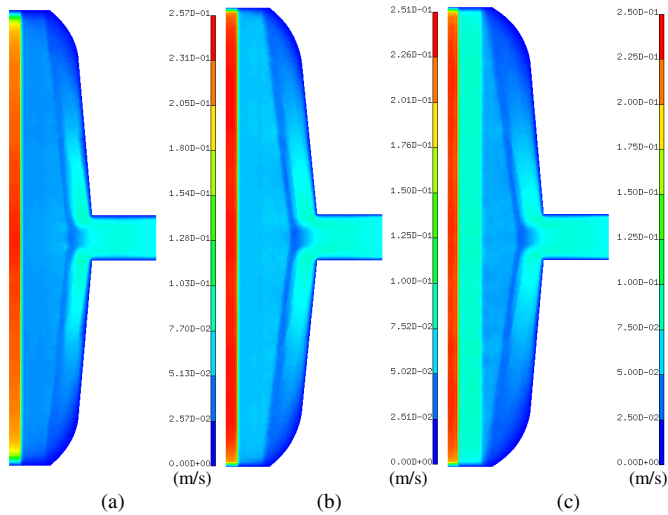


Fig. 3 Velocity distributions in the mid-plane of the initial (a), intermediate (b), and optimized (c) designs of the flat die.

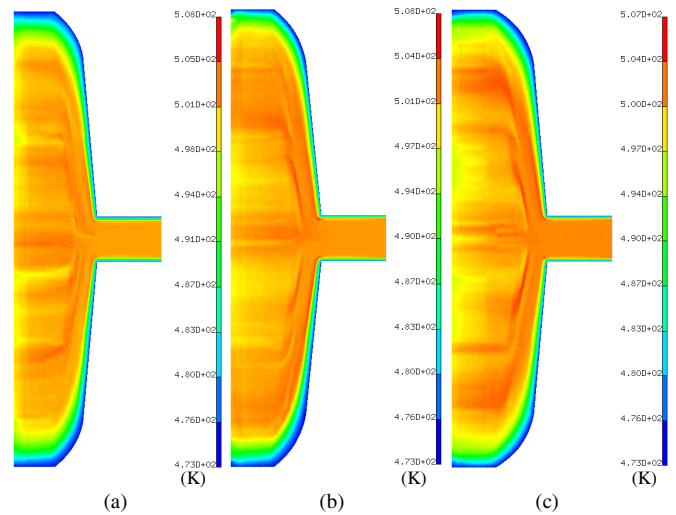


Fig. 5 Temperature distributions in the mid-plane of the initial (a), intermediate (b), and optimized (c) designs of the flat die.

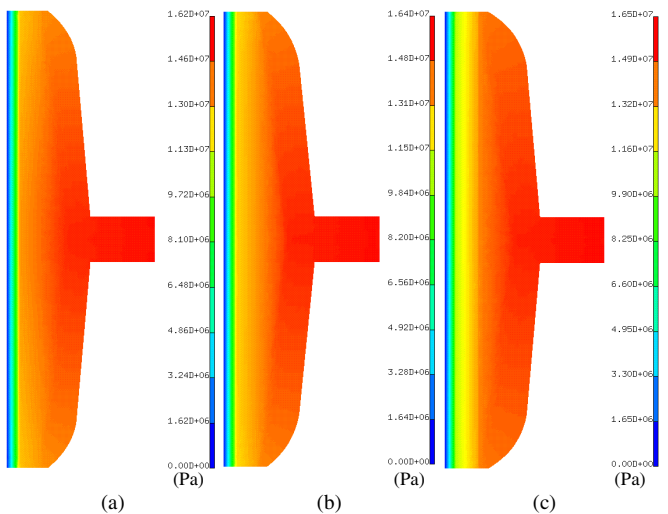


Fig. 4 Pressure distributions in the mid-plane of the initial (a), intermediate (b), and optimized (c) designs of the flat die.

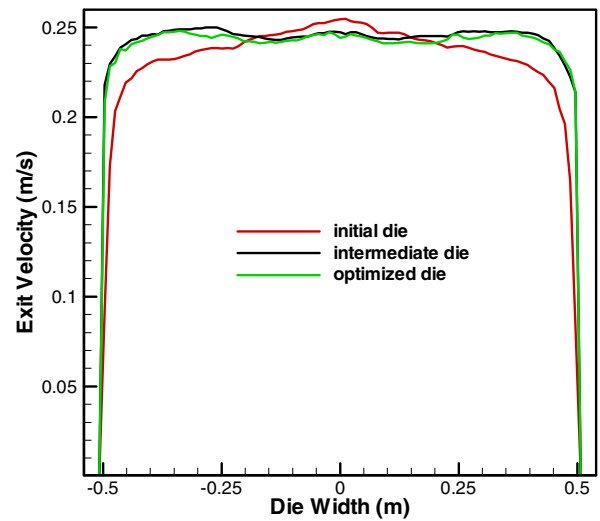


Fig. 6 Exit velocity across the width of the flat dies.